IEEE ComSoc IEEE Open Journal of the Communications Society

Received XX Month XXXX; revised X Month XXXX; accepted XX Month XXXX. Date of publication XX Month XXXX; date of current version XX Month XXXX.

Digital Object Identifier 10.1109/OJCOMS.2025.1234567

Toward Sustainable Future Wireless Networks: Power Reduction and Energy Harvesting Strategies

MICHAEL C. PARKER[1], SENIOR MEMBER, IEEE, GEZA KOCZIAN[1], MANOJ THAKUR[1], NABEEL NISAR BHAT[2], JAKOB STRUYE[2], JOSHUA JALALI[2], OZGUR OZKAYA[3], JETMIR HAXHIBEQIRI[3], ABDULHALIM FAYAD[4], STUART D. WALKER[1], JEROEN HOEBEKE[3], TIBOR CINKLER[4], AND JEROEN FAMAEY[2]

[1]School of Computer Science and Electronic Engineering, University of Essex, Colchester, UK
[2]University of Antwerp - imec, Belgium
[3]University of Ghent - imec, Belgium
[4]BME: Budapest University of Technology and Economics, Budapest, Hungary

CORRESPONDING AUTHOR: Michael C. Parker (e-mail: mcpark@essex.ac.uk).

IEEE OJAP encourages responsible authorship practices and the provision of information about the specific contribution of each author.

This work was funded by the CHIST-ERA SAMBAS, Sustainable and Adaptive Ultra-High Capacity Micro Base Stations project. This work was partly funded by the Engineering and Physical Sciences Research Council (EPSRC) under grant EP/W03560X/1 (SAMBAS-Sustainable and Adaptive Ultra-High Capacity Micro Base Stations). Nabeel Bhat is supported by the Fund for Scientific Research Flanders (FWO) under grant agreement number 1SH5X24N.

ABSTRACT As the demand for mobile connectivity continues to rise — both in terms of user densities and data throughput — the energy consumption of next-generation mobile networks is on the increase is only expected to become even larger in 6G. This trend is further intensified by the shift to higher-frequency bands and the deployment of a larger number of physically-smaller and lower geographical coverage base stations. In this paper, we propose a set of novel approaches, developed within the CHIST-ERA SAMBAS project (*"Sustainable and Adaptive Ultra-High Capacity Micro Base Stations"*), to improve energy efficiency in next-generation mobile networks. On the one hand, we aim to reduce the overall energy consumption of mobile networking; on the other, we explore the substitution of a significant portion of energy demand with green, locally harvested renewables — either used instantly or stored for later use - made practicable by the powering requirements of smaller yet still high-performance micro-base stations. We also introduce models, strategies, and methods, accompanied by a comprehensive assessment of their performance and feasibility.

INDEX TERMS Energy efficiency, wireless networking, reflective intelligent surfaces, sustainability, network re- source allocation, locally harvested renewable energy, green energy, green networks, mmWave, micro base station.

I. INTRODUCTION

Sixth generation (6G) wireless networking research is rapidly progressing as fifth generation (5G) technologies are now mature and widely deployed. By improving radio technologies and using higher frequencies such as millimeter wave (mmWave) and higher (THz) bands, 6G aims to meet growing communication demands. However, this potentially comes with high energy costs. Technologist Peter Cochrane has described 5G as "the most energy-hungry and wasteful mobile technology ever," with some cell towers consuming over 10kW and overall consumption projected to rise 61-fold from 2020 to 2030 [1], [2]. As 6G expands into private and industrial environments (e.g., Industry 4.0), energy use is expected to rise accordingly, such that sustainability must therefore be made central to 6G development.

Energy-efficient (low-power) wireless telecommunications has therefore become a central research theme because network capacity growth (more sites, more spectrum, more antennas, more devices) can otherwise drive power consumption and operating cost upward. It's already well known that designing from the outset an energy-efficient communications system represents a multi-variate optimisation problem, requiring a set of trade-offs, e.g. between spectral efficiency and energy efficiency, deployment density and energy efficiency, bandwidth and transmit power, and delay/latency versus power, such that improvements need to be evaluated at the *system* level rather than by link budget alone [3].

To this end, typical measures of energy performance using metrics such as Joules/bit (or bits/joule), or even fundamental (entropy-based) thermodynamic measures that are logarithmic and indicate the multi-orders of magnitude in improvements that may possibly be attained [4]. This also emphasizes that

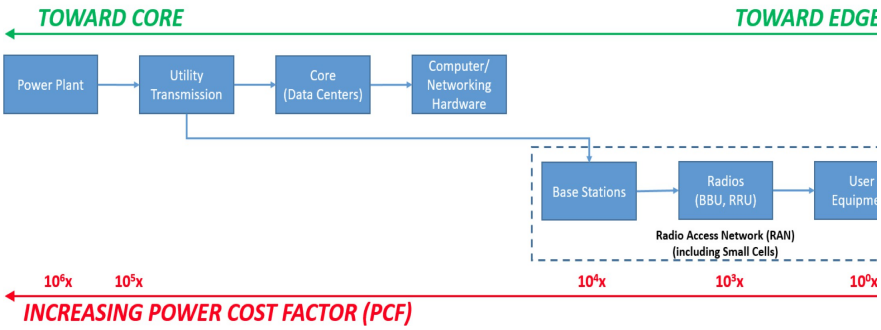

FIGURE 1. 6G power value chain, e.g. [17].

circuit and infrastructure power (RF chains, baseband processing, cooling, backhaul/fronthaul) often matter as much as radiated power. The whole green telecoms field has been consolidated already for the past decade into a toolbox spanning PHY/MAC co-design, resource allocation, network architecture, and hardware-aware modelling [5-7].

At the radio access layer, massive MIMO was an early solution to improve power efficiency: by coherently focusing energy and exploiting array gain, the power required to transmit power for a target rate can be reduced to improve energy efficiency—provided the extra circuit power and signal processing overhead are accounted for [8]. In parallel, the densification of small cells and heterogeneous networks has also shifted attention to traffic-adaptive operation: switching off or "dozing" base stations and coordinating among neighbouring cells to deliver large savings during off-peak periods without unacceptable coverage or QoS loss [9,10].

At the architecture design level, centralization and coordination have been exploited to introduce opportunities for both energy and costs (CapEx and OpEx) reductions. In Cloud-RAN, coordinated beamforming and remote radio head selection can reduce *network* power by jointly optimizing radio transmission and transport power [11]. Similarly, cell-free massive MIMO (many distributed access points jointly serving users) has been analyzed under "total energy efficiency" models that include channel estimation, power control, hardware power, and backhaul power—highlighting when a distributed architecture's spectral gains do (and do not) translate into net energy gains [12].

Another important approach for energy-efficient wireless transmission is to reshape propagation rather than only increasing transmit power, and this has led to the emergence of Reconfigurable Intelligent Surfaces (RISs) as a means to improve link quality and coverage with low-power, largely passive elements, enabling energy-efficient designs that jointly optimize transmit precoding and RIS configuration [13].

Low-power networking is increasingly intersecting with energy harvesting and wireless power transfer as the appropriate energy extraction and storage technologies have matured. Recent RF energy harvesting surveys and JSAC reviews show how "energy-neutral" operation can be approached for IoT and sensor-class devices, but also emphasize the new constraints (stochastic energy arrival, storage limits) that reshape scheduling, coding, and network control [14,15]. Underpinning many of these advances is a mature optimization viewpoint: energy efficiency problems are commonly fractional (rate/power), motivating algorithmic frameworks that make such objectives tractable in multiuser, interference-limited systems.

RF energy harvesting is a low-power technology (typically in the μW-mW regime) which represents an important adjunct renewables technology as compared to the higher power sustainable and energy-harvesting strategies being discussed in this paper. More specifically, an RF energy-harvesting antenna can be used to wake up dormant devices that are operating in a zero-powering sleep mode. For example, a remote BS device relies on a renewable powering source when operating in its normal functioning mode as a base station, and also has a battery back-up in conjunction with its renewable source (e.g. a solar panel). However, when in a dormant mode for an extended period, rather than drawing on a small amount of battery power, it can operate in a completely zero power mode (conserving all available battery power), and then be activated (switched on) by a pulse of RF energy received at its antenna. After having been switched-on using the RF energy harvested from the antenna it can then switch to the larger powering afforded by the battery and other sustainable sources. The mathematical model for RF energy harvesting is non-linear in nature since the powering output depends on the radio signal strength, which represents a stochastic quantity, being highly dependent on local environmental factors such as the meteorological state and amount of precipitation and moisture in the air, the presence of moving obstacles in the vicinity blocking or modifying the line-of-sight path from the RF source, and the local topography of the terrain.

Recent advances in battery technology are also indicating that sodium-based (as opposed to the more conventional lithium-based) battery technologies are particularly suitable for remote devices in hostile environments. In particular, sodium batteries are much more rugged, being able to tolerate a far greater temperature range than lithium-ion batteries and can also endure being left flat for long periods of time. It is also noteworthy that sodium represents an inherently more sustainable, cleaner and economic technology than lithium.

Although efforts are underway to develop zero-energy end-devices [16], this only addresses a small part of the total energy chain (see Figure 1). Energy usage increases

significantly closer to the network core, where fewer but more power-intensive components are found. Both communication and computation infrastructures — from edge nodes to data centers — currently consume large amounts of energy, even when idle. Therefore, optimizing energy use beyond end devices is essential, with a focus on the powering of the infrastructures supporting them of specific interest.

Prior research has addressed energy efficiency through various mechanisms. For instance, [10] explored sleep-mode strategies in macro-base stations, achieving 10% savings. Similarly, [14,15] proposed energy harvesting for IoT devices, though their approach lacks scalability for mmWave µBSs. Recent surveys on AI for green communications [18] suggest that reinforcement learning is promising, yet few studies have validated this on real-world 60GHz hardware.

Most studies focus on simulation or lower frequencies; few address the specific power dynamics of mmWave/THz µBS powered by renewables.

We briefly consider here the key characteristics of the renewable sources of energy available to make future 6G networking more sustainable, and where specific innovations to improve their power efficiency and energy harvesting performance are currently active research topics:

- *Photovoltaics/Solar* – Recent advances in new material designs (such as perovskite-silicon architectures) have made solar panels much more efficient, with laboratory efficiencies now approaching the intrinsic efficiency limit of ~40%. PV panels operating at infrared wavelengths now also allow them to operate at night-time and offer some useful nocturnal powering functionality. The electrical impedance of PV panels is a straightforward electrical issue, which can also be dynamically optimised using electronics to maximise the output power whatever the variable local conditions of illumination.
- *Wind* – Wind turbines can easily generate kW's of power, but are highly dependent on the local wind conditions such that peak output power will often be a rare event (particular for land-based wind turbines), with hilltops (rather than urban settings) and ridges the optimum land-based locations best place to harness katabatic winds. The key issue is that wind turbines are not reliable (i.e. they are highly stochastic) such that local energy storage is required, both to absorb the peak powers when not all of it is immediately required and to release power when insufficient is being generated by the turbine. The characteristic aerodynamic impedance of a turbine can be modelled as a simple Thevenin equivalent circuit (voltage sources in series with a resistor) with the resistor being varied to offer dynamic and complex (i.e. real and imaginary) behaviour so as to optimise impedance matching (and maximise power transfer). Particularly for a wind turbine the output voltage is frequency dependent and will vary as the speed of the rotor changes according to wind conditions. Particularly for wind turbines, the maximum power point tracking (MPPT) needs active control so as to avoid stalling at low speeds, where varying the aerodynamic impedance of the turbine according to the wind speed is a simple electronics control problem that can be employed to avoid stalling. In addition, for high wind speeds where there might be the risk of turbine burn-out, the introduction of complex values for the aerodynamic impedance can also enable the rotor speed to be safely reduced (by reactive braking) and avoid operation beyond the safe limits of the turbine's operational envelope.
- *Hydro* – Hydraulic turbines have a similar characteristic to wind turbines, with the key difference being due to the high density of water as compared to air: factor ×1000. This means that a hydraulic turbine (e.g. located in a river) can give continuous large output powers, according to the hydraulic pressure and water velocity. The characteristic hydraulic impedance is not due to the winding resistance of the turbine, but according to the Betz equation is found to be inversely proportional to the water speed. Again, stalling is an issue at lower water velocities, but passive and simple electronic control can also be used to dynamically vary the hydraulic impedance to avoid stalling and also ensure operation at the MPPT. We are currently investigating new models of frequency-based impedance matching (currently neglected) so as to optimise power output of hydraulic turbines.

6G is expected to deliver ultra-fast data rates (over 1 Tb/s), low latency, and massive device connectivity, enabling innovation in sectors such as healthcare, autonomous transport, immersive media, and smart manufacturing [17], [19]. In this context, the SAMBAS initiative ("Sustainable and Adaptive Ultra-High Capacity Micro Base Stations") proposes a holistic, sustainability-first approach across radio, networking, and service layers. SAMBAS tackles three core 6G challenges:

- Moving beyond always-on mmWave hardware toward energy-efficient components with energy harvesting;
- Replacing energy-intensive, centralized networks with decentralized, context-aware energy management and intelligent scheduling;
- Joint optimization of hardware, networking, and resource allocation to improve sustainability, rather than treating them in isolation.

From a theoretical perspective, using the results emerging from the SAMBAS project, this work introduces: (i) analytical power consumption models for mmWave µBSs under different operational states, (ii) a formal Green Energy-Aware User Assignment optimization problem, (iii) an ILP formulation for joint user association and µBS activation, and (iv) a fractional non-convex optimization framework for THz UAV-assisted NOMA-SWIPT networks. Thus, this paper presents results that are experimental as well as theoretical (based on both observational as well as simulation-based outputs) highlighting the theoretical and mathematical formulations that are required to underpin an effective energy-efficient 6G networking framework. We show that

sustainability requires appropriate intervention at the hardware (renewables/harvesting), network strategy (sleep modes/planning), and edge applications (UAV/SWIPT) levels.

It's worth nothing here that the higher modulation and coding scheme (MCS) discussed here reduces energy due to a reduced transmission/receiver occupancy time, while single-connectivity minimizes µBS activation count, and hence power. Both these points are theoretical findings and not just empirical observations. Likewise, we note that since the SAMBAS project is a multi-partner enterprise, this paper represents the results of multi-technology integration efforts, covering multiple topics, each if which embodies an important component of any comprehensive energy-efficient 6G solution. In so doing, we have endeavored to write a coherent, yet inevitably partial account of the current strategies to achieve low energy 6G networking, which connects the dots between the various available technology choices, so as provide an understandable overview of what is practically possible for a sustainable future 6G network.

The paper is structured as follows: Section II presents energy harvesting models and measurements for micro-base stations (µBSs) with a system-level power consumption model and a renewable-aware user assignment optimization problem. Section III explores energy-aware radio access network (RAN) scheduling and resource allocation by formulating the energy-efficient user association problem as an ILP under QoS and connectivity constraints. Section IV describes a demonstrator using unmanned aerial vehicles (UAVs) and various energy-reduction techniques. The UAV-assisted network is modeled as a fractional non-convex optimization problem, solved via successive convex approximation and quadratic transformations. Conclusions follow in Section V.

II. Energy lifecycle modeling and prediction for green networks

A. ENERGY HARVESTING SOLUTIONS FOR SUSTAINABLE WIRELESS NETWORKING

Enhancing the energy efficiency of mmWave µBS systems is critical for sustainable 6G networks. Recent artificial intelligence (AI) and machine learning (ML) advances support integrating renewable energy harvesting with intelligent power management and communication protocols. This work focuses on real-time µBS energy automation, adapting power usage to traffic and energy availability. Using LoRaWAN, 100-watt solar panels, and EcoFlow batteries, we demonstrate scalable, self-sustaining µBS systems that minimize energy consumption while maintaining performance.

We note here that the although in this experimental work the physical footprint of the renewable energy setup may be considered large (alongside the required storage battery), this is more a result of the practical limitation of the available demonstration capabilities; whereas a more optimal dimensioning of solar panel and storage is also accessible for any widespread deployment, as has been verified using the simulation techniques (e.g.) as outlined later in this paper.

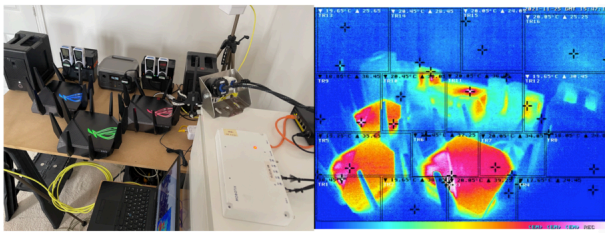

FIGURE 2. Experimental Temperature Monitoring of µBS components using the MOBOTIX S74 camera.

In this work, AI techniques are used at three distinct levels: (i) rule-based and predictive analytics for real-time energy control in experimental µBS testbeds, (ii) learning-assisted optimization (genetic algorithms) for network-level resource allocation, and (iii) mathematical optimization frameworks that provide theoretical performance bounds. Deep neural network-based learning is discussed as enabling extensions but is not the primary focus of the current implementation.

The architecture enables up to 500 internet of things (IoT) devices per LoRaWAN gateway, with AI systems dynamically managing power during traffic peaks and low renewable input, thereby reducing waste and achieving 15–20% energy savings. Real-time data from TP-Link Kasa smart plugs support adaptive control, keeping router powering between 12.5–13.4 W and NAS power stable at 49.5 W. Indoor and outdoor testbeds were used to validate the system's effectiveness.

1) The Role of AI in Green Wireless Communications: AI (including ML and deep learning architectures) optimizes telecom energy use by learning from historical and real-time data, predicting demand, and making intelligence-based decisions. Predictive analytics help adjust loads during peak/off-peak times, while reinforcement learning enhances routing and spectrum use, with deep learning aiding anomaly detection, and reducing waste from faults or security issues.

AI also improves integration of renewables via forecasting and smart storage management, aligning tasks with energy availability. Adaptive beamforming and load balancing can also be used to reduce signal loss and infrastructure strain, with AI switching idle components to sleep mode, to further improve efficiency.

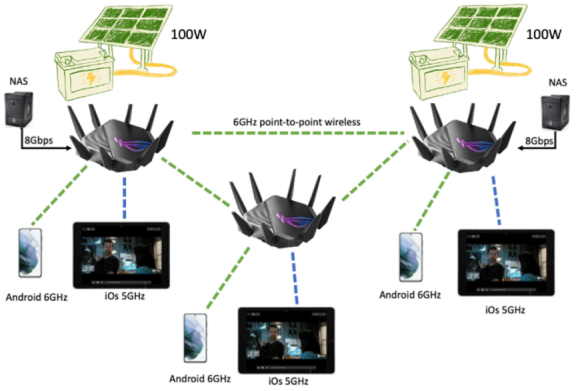

FIGURE 3. Energy harvesting for 6G experimental setup.

Edge intelligence enables local processing, reducing transmission loads and latency, such that AI can also adjust IoT transmission intervals and power levels based on battery and network conditions, to ensure network-wide efficiency.

2) AI-driven Energy Optimisation in Next-Generation Wireless Networking: The sustainable wireless network described here uses AI-based power management to optimize router and NAS power based on real-time plug data. Adjustments during low traffic or poor solar input yield 15–20% savings without performance loss, with historical trends also allowing proactive configuration optimisation. Thermal data from MOBOTIX S74 cameras additionally enable predictive cooling, to ensure the µBS components remained within safe operational limits even under heavy workloads. The AI-driven controller relies on light touch predictive analytics using historical power consumption and solar generation data. Regression-based forecasting and adaptive thresholding are used to adjust router transmit power, MAC parameters, and sleep states in real time. While deep learning methods are applicable, the current implementation prioritizes explainability and low computational overhead suitable for edge deployment. It's also clear that optimising (lowering) powering requirements for network equipment also lowers the required dimensioning of the associated energy harvesting and storage technologies.

The hardware assembly involved connecting the 100-watt solar panels to the EcoFlow battery using standard solar charging cables. The Asus GT-AXE11000 router and Network-Attached Storage (NAS) were connected to the battery using TP-Link Kasa KP115 and HS300 smart plugs to monitor their power consumption.

In this paper, we combine experimental measurements and simulation-based evaluations. Experimental results are obtained from real-world µBS energy-harvesting testbeds and mmWave power measurement setups. Simulation results are produced using ns-3 and custom optimization frameworks to evaluate large-scale network behavior and hypothetical deployment scenarios. The software setup included installing Python and the necessary libraries, such as asyncio, psycopg2, and dash, on the monitoring computer, while the PostgreSQL database was configured to store time-stamped energy metrics, while Python-based monitoring scripts were deployed to asynchronously collect data from the smart plugs, thereby allowing continuous real-time data collection and storage.

For data visualization, a customisable Dash-based web dashboard was employed to display energy usage metrics, including current, voltage, power, and total energy usage for each device. LoRaWAN sensors were deployed at varying distances to gather environmental data and test communication performance, with RSSI and SNR values recorded under different line-of-sight and non-line-of-sight conditions, allowing for a comprehensive assessment of the network's performance across diverse environments.

3) Energy harvesting experimental set-up: Figure 3 shows the µBS energy harvesting setup with 100-watt monocrystalline panels connected to EcoFlow batteries. Positioned at optimal tilt, they deliver 70–80 W in sunlight and 20–30 W in low light. Batteries recharge to 99% in 6 hours and provide consistent power, ensuring performance despite varying external operating conditions.

Under full load, the battery's discharge rate remained consistent, supplying reliable power without significant voltage drops, with the system's design guaranteeing stable power, and thereby ensuring network performance even as the battery depletes and under changing environmental conditions.

The router's power consumption did not vary much with load, ranging from 12.5 W to 13.4 W depending on network activity and environmental factors. During high network traffic, power consumption approached the upper limit due to increased processing and wireless transmission demands, while during low traffic periods, consumption remained closer to 12.5 W. The NAS system consistently drew between 49.5 W and 49.9 W, again reflecting stable operation regardless of network conditions. Predictable energy requirement also aids efficient energy management. Nevertheless, accurate power consumption measurement is critical for optimizing the µBS system's energy efficiency.

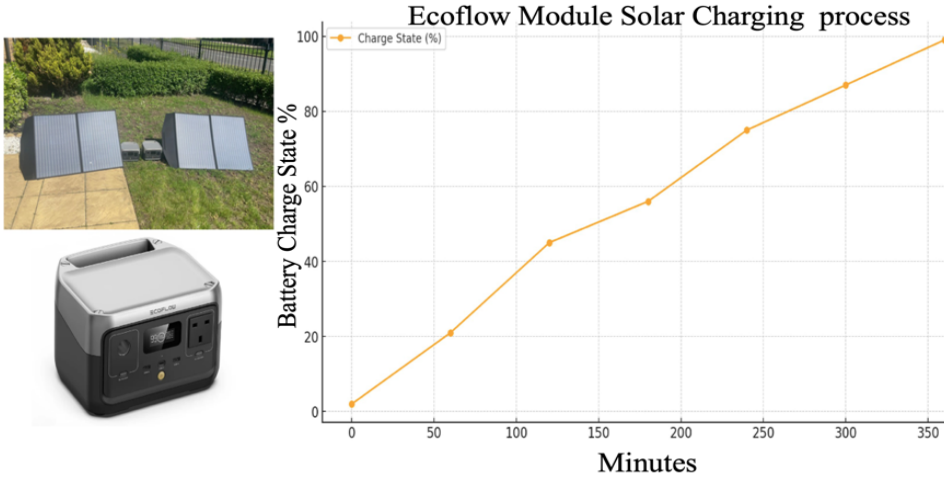

FIGURE 4. **EcoFlow Battery Solar Charging Process.**

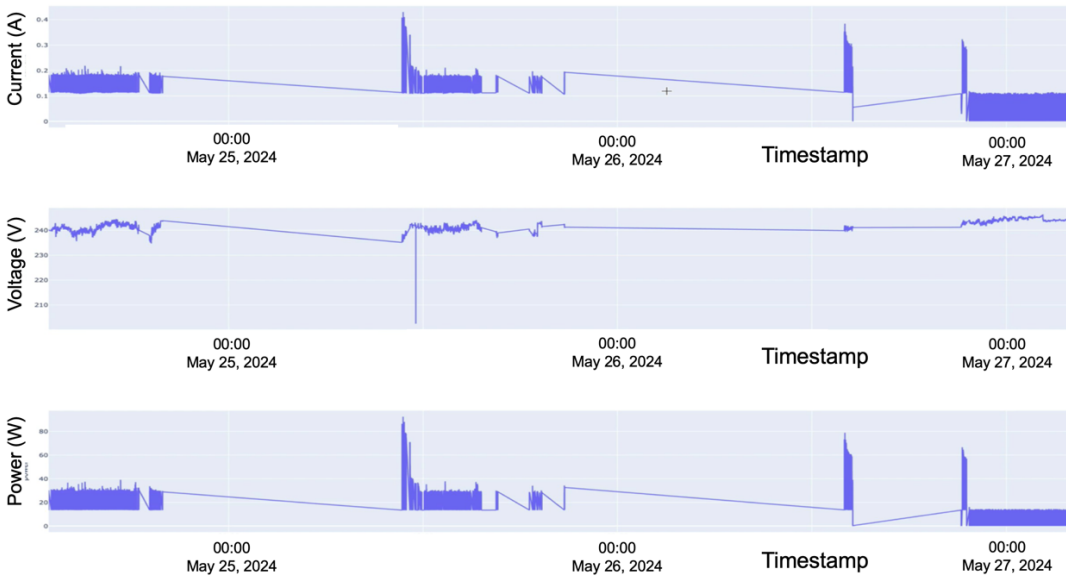

FIGURE 5. Historical energy consumption data illustrating patterns and informing AI optimizations.

System monitoring was achieved by a dedicated computer with Python 3.x installed, along with the Python libraries to record the relevant energy metrics, including fields for timestamp, device name, current, voltage, power, and cumulative energy. Monitoring scripts were developed using Python and asyncio to asynchronously collect data from the smart plugs at one-second intervals; the asynchronous approach ensuring continuous operation without interrupting other tasks. The retrieved energy data was stored in the PostgreSQL database in real time, providing a comprehensive overview of energy consumption, with data including current (amps), voltage (volts), and power (watts) to offer granular insights into energy usage.

4) Firmware integration of μBS: Firmware integration aimed to improve energy efficiency using off-the-shelf components. AI-controlled MAC protocol adjustments based on live energy and traffic data reduce retransmissions and power use. During low traffic, contention windows shrink for better throughput; during high traffic, they expand to reduce collisions. Transmission power was dynamically tuned based on solar input and battery levels, with the TP-Link Kasa plugs monitoring energy usage. Adjustments, such as reducing output from 12 dBm to 8 dBm, were able to preserve power without major performance loss. Remote SSH access enabled firmware modifications on the Asus GT-AXE11000 router.

5) Results of energy harvesting: Dash-based dashboards visualize real-time energy data from smart plugs, with graphs showing router and NAS power usage over time. Anomaly detection triggered automated corrections, such that the AI-informed adjustments achieved 15–20% power usage savings.

6) Automatic AI-Optimized Control of Overall μBS Powering: The AI system adapts power use to solar input and traffic, increasing powering during high load, and reducing it when idle. Bandwidth metrics help correlate traffic and energy use, with the AI continuously learning from the historical patterns to improve its forecasts. In tests, reducing router power from 13.4 W to 11.8 W caused minimal latency change (18 ms to 19 ms), confirming efficiency improvement with only minor performance loss.

B. POWER CONSUMPTION MEASUREMENTS OF mmWAVE μBS

This section analyzes the power usage of the mmWave μBS devices based on empirical data from commercial-off-the-shelf (COTS) hardware. We specifically evaluate the MikroTik wAP60Gx3, a 60 GHz IEEE 802.11ad device with 96 antennas and a 180-degree field of view. The data feeds into a simulation tool to estimate consumption across various scenarios. The proposed Genetic Algorithm (GA) acts as a learning-assisted optimization technique that iteratively adapts user association and μBS activation patterns based on observed fitness improvements, thereby approximating the optimal ILP solution with significantly reduced computational complexity. To achieve energy-efficient networking, we first formulated the user association problem as an ILP aiming at minimizing total grid power consumption subject to minimum bitrate constraints. Given the NP-hard nature of the ILP, we

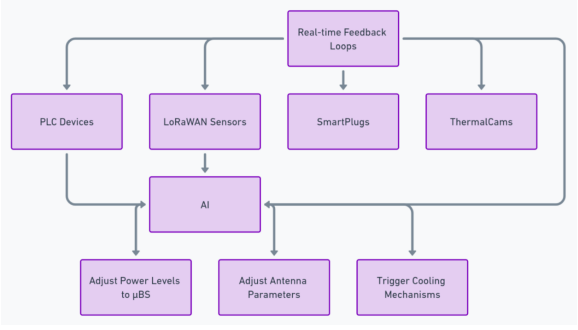

FIGURE 6. Diagram of the AI-driven power management system optimizing energy usage in real time.

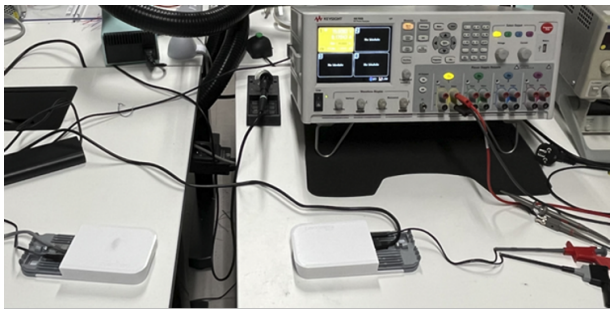

FIGURE 7. Power measurement setup with MikroTik wAP60Gx3 devices and Keysight analyzer.

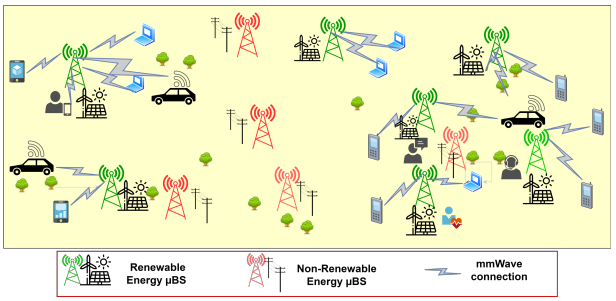

FIGURE 8. Example of a 6G wireless network deployment with integrating locally harvested renewable energy.

employed a GA, operating with a population size of 200, utilizing Roulette Wheel selection, and featuring a linear regression crossover operator (rate = 0.8) and an applied mutation rate of 0.02 to prevent local optima. The fitness of each individual was evaluated against the ILP objective function, and the energy availability at each µBS was determined by a Support Vector Regression forecasting model, which predicts harvested energy based on historical solar irradiance, time of day, and weather telemetry with an observed 10% accuracy. It may be noted that this is an experimental demonstration of a minimum-viable product (MVP) within the resources of a participating (university) partners, which is aimed at proving to TRL4/5 (i.e. laboratory validation) rather than TRL6/7 (which is demonstration in an operational, industrial environment) the validity of our approach remove. That is to say, we use simulation (see next section §2.C) to justify extrapolation to a large number of users in a practical deployment scenario, using the empirical results of a single user.

1) Empirical Power Measurements: We used two MikroTik wAP60Gx3 units—one as µBS, one as user equipment (UE)—and a Keysight N6705B Power Analyzer (10 µs sampling). Figure 7 shows the testbed. Devices were powered at 15 V, within their 12–57 V operating range, to measure current and compute power. The power consumption is measured in a variety of communicating and non-communicating states:

• **Not associated:** This state is the lowest power setting for the device. It indicates the minimum power that needs to be supplied to keep the devices on. Both µBS and client consumes an average power of 1.67 W with a peak value of 1.97 W.

• **Radio on:** This state represents the power consumed when the wireless interface on the device is turned on so that it can connect to an access point (AP). In this case, we measure an average value of 2.1 W with peak value of 2.34 W.

• **Scan:** This state represents the UE looking for available networks to connect to. The power consumption in the scanning state can go as high as 2.92 W with average value of 2.64 W. However, the scan duration is only 440 ms. The smaller number of channels at 60 GHz and small scanning time makes the overall scanning operation efficient compared to, for example, 5 GHz Wi-Fi.

• **Beacon Header Period:** We also measured power consumption during the beacon header period. During this period, the µBS periodically transmits beacon frames to announce its presence, allocates resources to UEs, and performs beamforming training. By default, the beacon header period occurs every 102.4 ms. However, the interval can be differently configured. The average power consumption within the beacon header period is 3.73 W with a peak value of 4.17 W. This is approximately twice the power consumption of the not-associated state.

• **Associated:** This means that the UE and µBS are connected; however, there is no exchange of traffic except the periodic control packets (e.g., beacons). For both types of devices, the power consumption values are very similar, with a mean power of 2.55 W for the µBS and
2.48 W for the UE respectively. The peak power can go as high as 4.2 W and 4.17 W respectively.

• **Transmission/Reception:** In this mode, we set up iperf to transmit a UDP data stream from the UE to the µBS at fixed data rates of 800 Mb/s and 500 Mb/s. For 800 Mb/s, the average power consumption at the receiver is 4 W, with a peak value of 4.3 W. At the transmitter side, an average value of 3.92 W and maximum of 4.39 W is recorded. In the 500 Mb/s case, the average values are 3. 6 W and 3.9 W for the receiver and transmitter respectively.

• **Idle state**: The idle state refers to the state following a packet transmission/reception. For both devices, the power drops

TABLE I. Summary of the power consumption measurement results using the MikroTik wAP60Gx3 devices, both in UE and µBS mode.

State	Device	Avg (W)	Peak (W)
Not associated	UE/µBS	1.67	1.97
Radio on	UE	2.1	2.34
Scan	UE	2.64	2.92
Beacon period	µBS	3.74	4.17
Associated/Idle	UE	2.55	4.2
Idle	µBS	2.48	4.17
Rx (500 Mbps)	µBS	3.6	3.9
Tx (500 Mbps)	UE	3.9	4.27
Rx (800 Mbps)	µBS	4.0	4.3

immediately to the associated values after packet transmission/reception.

Table I summarizes the power consumption measurement results of the UE and µBS in each of the considered states. The measured power values in Table I can be understood through the standard linear hardware power consumption model for wireless transceivers, where total device power is decomposed as $P_{total} = P_{circuit} + P_{RF}$. Here $P_{circuit}$ represents static and dynamic circuit power (baseband, oscillators, mixers, LNAs) and P_{RF} is the RF front-end draw during transmission. When idle only minimum circuits are active to sustain functionality, yielding $P_{min} \approx 1.67$ W. When communication is desired, the 60 GHz phased-array front-end needs to be optimized (which requires additional power) and which adds $\Delta P_{LO} \approx 0.43$ W. During the final optimization a mean power of 3.74 W is required; approximately double the idle power. During active Tx/Rx at 800 Mbps the more sophisticated transmitted data format requires more digital processing and a higher PA output, increasing to 4 W. The small difference in 500 Mb/s transmission reflects near-constancy in PA efficiency. Table II (below) follows a monotonically decreasing trend with increasing MCS, consistent with time spent in the active Tx/Rx state.

2) Power Consumption simulation results: From Table I, we can estimate network power usage for applications using similar mmWave hardware, based on time spent in each device state. Accurately determining these fractions is complex due to dependencies like data rate, beamforming, modulation and coding scheme (MCS), retransmissions, and mobility. To simplify, we evaluate a specific application using the ns-3 simulator, which supports IEEE 802.11ad/ay [21] and energy tracking.

We simulated mobile Virtual Reality (VR) to represent a demanding mmWave use case. Since VR headsets (UE) are energy-constrained, we also focus on receiver-side metrics. In addition, because retransmissions are less relevant in low-latency VR, all data must be delivered on time, such that we also built a new ns-3 app to send fixed-size data bursts at configurable rates and intervals.

Using ns-3's mobility module, the UE moves from 1m away at 0.5m/s in a straight line, and beamforming stability is maintained to avoid data loss due to null zones between adjacent beams. Data rates of 400, 1000, and 2350Mb/s represent the advanced 4K and extreme 8K VR cases [22].

MCS strongly impacts energy use so a higher MCS reduces energy due to reduced Tx/Rx occupancy time. We therefore simulated static and mobile scenarios (up to 15m and 25m) for even-numbered MCS up to 12, and with auto-rate adaptation. Mean energy is reported only when links remain stable, with the results shown in Table II below.

As expected, power use declines as MCS increases, since higher MCS shortens receive time. Lower MCS can't meet higher data demands, and upper MCSs struggle at longer ranges due to SNR limits. For each scenario except for 2350Mb/s at 25m, there was at least one functional MCS at any point.

Rate adaptation (i.e., automatic MCS) consistently performs best as it operates by adjusting to SNR conditions. Although IEEE 802.11ad/ay doesn't define a standard algorithm, our simulation uses ns-3's default [21]. Notably, MCS12 mode and rate adaptation save 24.5% over MCS4 at 1000Mb/s static, highlighting that idle radios only consume ~ 35% less power than active ones.

Mobility doesn't affect power when the MCS is fixed, as long as the link holds. However, with automatic adaptation distance alters MCS selection and thus power use.

C. ENERGY PREDICTION MODELS FOR ENERGY HARVESTING

As already discussed, renewable energy is becoming integral to 6G network design, with solar, wind, and hydro offering viable, sustainable power sources for telecoms infrastructures under active consideration [18]. Here we use a prediction model based on the MVP-setup previously discussed, to provide simulated scaled-up network energy prediction and thereby enable hardware performance optimisation (lower powering needs). In this case, the MVP data is provided as parametric input in conjunction with expected demand curves.

SAMBAS capitalizes on the lower powering needs of micro base stations (µBSs) by using energy harvesting and smart control strategies to manage grid-connected units. These µBSs can switch on or off based on live traffic and energy availability to boost efficiency. In Fig. 8, red µBSs are grid-powered, while green ones run on renewables. In the shown

TABLE II. Power consumption results for download VR streaming application, simulated using the ns-3 network simulator, for different MCS values, maximum distance, and application data rate.

MCS	400 Mbps			1000 Mbps			2350 Mbps		
	Static	15 m	25 m	Static	15 m	25 m	Static	15 m	25 m
2	3.36 W	3.36 W	3.36 W	/	/	/	/	/	/
4	3.11 W	3.11 W	3.11 W	3.55 W	3.55 W	3.55 W	/	/	/
6	2.98 W	2.98 W	2.98 W	3.55 W	3.55 W	3.55 W	/	/	/
8	2.86 W	2.86 W	/	3.23 W	3.23 W	/	/	/	/
10	2.79 W	2.79 W	/	3.08 W	3.08 W	/	3.72 W	3.72 W	/
12	2.73 W	/	/	2.92 W	/	/	3.35 W	/	/
Auto	2.73 W	2.74 W	2.79 W	2.92 W	2.96 W	3.08 W	3.35 W	3.44 W	/

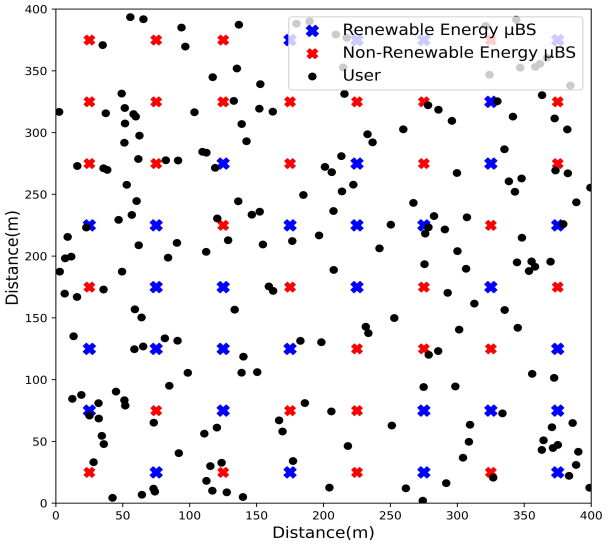

FIGURE 9. Example of Users and µBSs distribution for 200 users and 50% renewable energy.

setup, only the renewable-powered µBSs serve users, thereby reducing grid dependence. We consider ten types of µBS configurations, as defined in the following subsection.

1) Powering Classifications of µBS Deployment and Operation: The power source of µBSs directly affects their reliability, sustainability, and functionality. Reliability is particularly dependent on the continuity of the powering source, with renewable sources varying in their outputs due to the vagaries of environmental conditions, the storage battery potentially running out of charge, and diesel generators running out of fuel, while non-renewable (grid-connected) sources offer the most reliable powering, yet with the least green sustainability. We define the powering of the base stations to fall into ten categories, ranging from fully off-grid renewables to continuous generator supplied:

1) **Battery-less local renewables:** No storage; powered only by local energy.
2) **Local renewables with storage:** Fully off-grid with battery storage; assumed sufficient for full-time operation.
3) **Partial local renewables, no storage (grid-connected):** Uses some local energy but relies on the grid without storage.
4) **Partial local renewables with storage (grid-connected):** Uses local energy and storage, with grid backup.

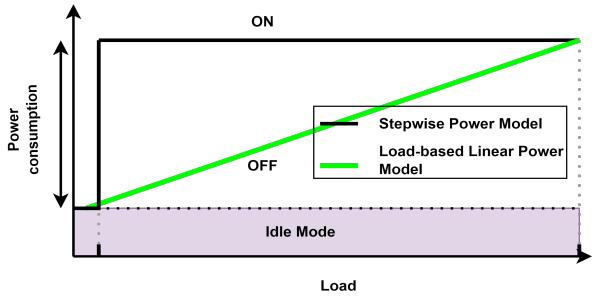

FIGURE 10. µBS power consumption model.

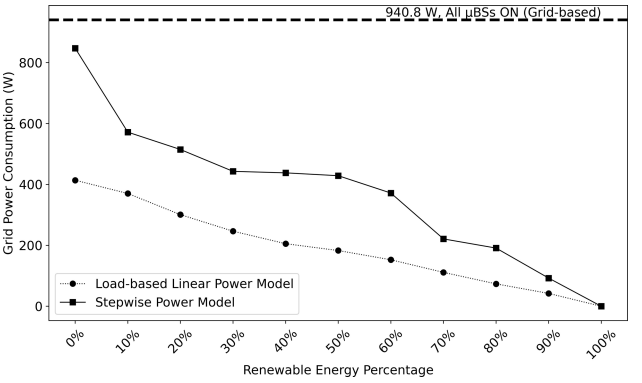

FIGURE 11. Grid Power Consumption of Load-based linear vs stepwise power model for 400 users.

5) **Non-local renewables (grid-connected):** Powered by offsite renewables via the grid.
6) **Fully grid-powered, no backup:** No batteries; relies solely on the grid.
7) **Fully grid-powered with UPS:** Has a small UPS battery for temporary backup.
8) **Battery-only (limited):** Powered by rechargeable batteries; runtime is limited.
9) **Mixed sources with generator and storage:** Uses grid, generator, and minimal storage.
10) **Diesel generator only:** Runs solely on a continuously operating generator.

2) System Model: We consider a set of µBSs, S, uniformly deployed over area A. This set is split into S_1 (powered by renewables) and S_2 (grid-powered), with $S_1 = \eta \cdot S$, where $\eta \in [0, 1]$ denotes the renewable fraction. µBSs in S_1 draw no grid power, i.e., Power(µBS) = 0 W. We also define a user set U that is uniformly distributed across the area.

Fig. 9 shows an example configuration: red 'X' = grid µBS, blue 'X' = renewable µBS, and black dots = users.

This work seeks to minimize grid dependency while maintaining service quality, such that we define this as the Green Energy-Aware User Assignment optimisation problem.

3) Power Consumption Models: We consider two µBS power models: a linear load-based model and a stepwise model. In the load-based model, the µBS power scales with

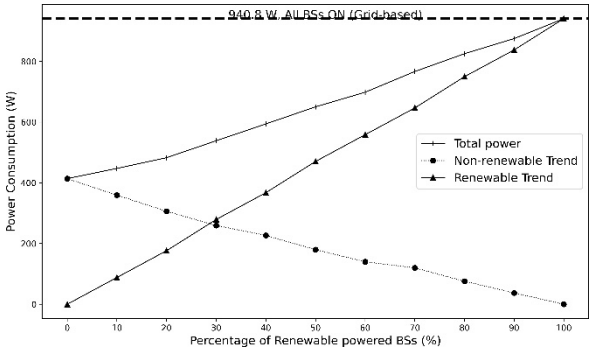

FIGURE 12. Network power consumption trends considering renewable and grid power sources for 400 users.

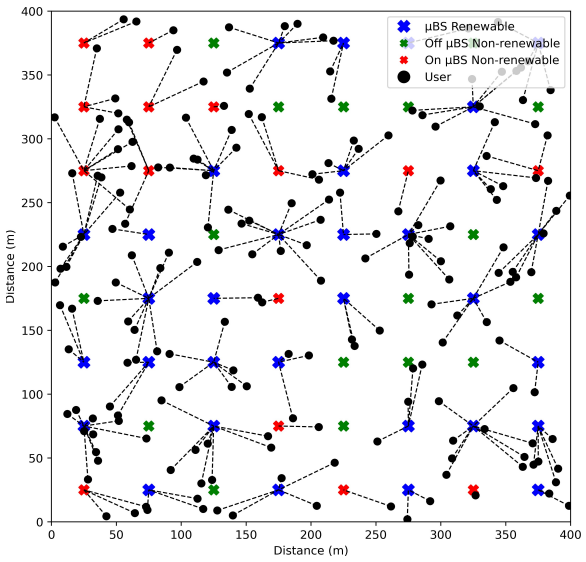

FIGURE 13. Users-μBSs configuration where 50% of μBSs are powered by renewable energy sources.

user load, increasing gradually with traffic. This reflects dynamic energy use based on service demand. In the stepwise model, μBSs draw full power when active (with at least one user) and none when idle. Power use is binary — "on" or "off" — ignoring user count beyond zero. These models are visualized in Fig. 10.

4) Simulation results: We simulate a wireless network with 64 μBSs in a 400 m × 400 m area, with a 50 m maximum inter-μBS distance. The system uses the 28 GHz mmWave band and 1.2 GHz bandwidth. Path loss uses a 1-metre reference point, assigning a baseline loss of 61.4 dBm, with a propagation exponent of 2.1. μBSs are assumed to have peak 30 dBm transmit power with a 5.8 variance for the power fluctuations, while antenna sizes are 0.1 m (Tx) and 0.01 m (Rx). Active power is set to 14.7 W, idle 4.3 W [23], and each μBS serves up to 30 users each with a minimum 20 Mb/s.

Fig. 11 compares three strategies: load-based, stepwise, and always-on. With 400 users and renewable integration from 10–100%, stepwise cuts power use compared to always-on, especially under low load, but still consumes up to 50% more than the load-based model.

Fig. 12 shows power consumption trends as the renewable μBS proportion rises. Grid energy falls from 413.9 W to near-zero, while renewable use grows to 940.8 W. Total energy use increases, but this shift reduces grid dependency. The dashed line at 940.8 W is the all-grid baseline. Despite higher overall energy, renewable integration benefits operators by reducing reliance on conventional sources.

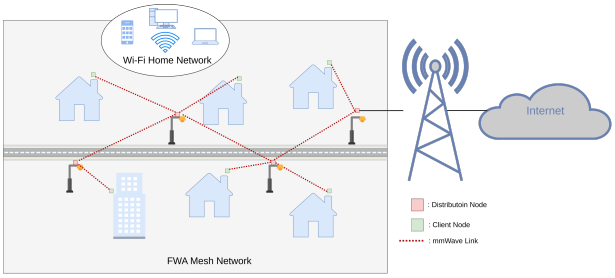

FIGURE 14. Illustration of a distribution access network including DNs and CNs.

Fig. 13 shows user-to-μBS allocation with 50% renewables. Green Xs: deactivated grid μBSs; red Xs: active grid μBSs; blue Xs: renewable μBSs; black dots: users. Connections favor renewable μBSs, using grid ones only when extra capacity is needed.

The distributions in the graphs reflect the difficulty of maintaining communication under a wide variety of circumstances: the wireless medium itself varies, interference is an unpredictable addition (Rician), circuit noise being both Gaussian and Poisson, the sophistication of the data beam being transmitted is variable to get maximum performance for a given power, and the protocol interchanges between μBS and end-user are all stochastic processes. As the total performance depends on a convolution of distributions, generally a central tendency can be assumed.

III. RAN ENERGY REDUCTION SOLUTIONS

Having examined energy consumption traits of individual 6G components and deployment strategies to minimize power use, we now focus on network-level strategies for reducing power demand. Within SAMBAS, where dense μBS deployment ensures 6G performance, coordinating these nodes in a RAN becomes vital for enhancing energy efficiency.

A. Coordinated schedule for energy-aware meshing

Wireless mesh networks (WMNs) are multi-hop, adaptable networks where routers extend coverage, gateways link

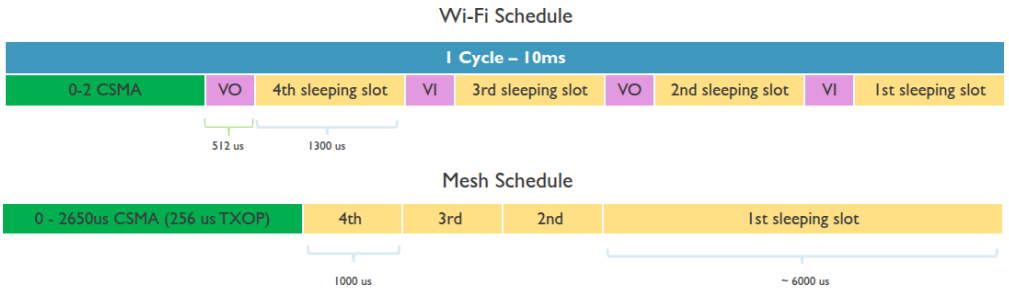

FIGURE 15. Schedules used in Wi-Fi and Mesh Network. Thanks to having a higher data rate in mmWave mesh network, it is possible to sleep more without harming networking services. CNs.

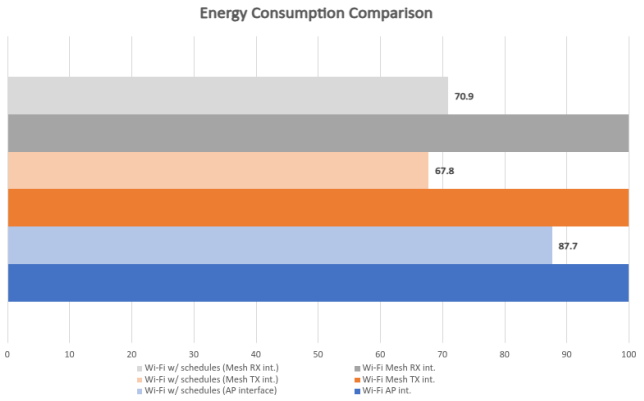

FIGURE 16. Energy consumption comparison between vanilla Wi-Fi and Wi-Fi with schedules when 8 TC applications are considered.

external networks, and clients connect via devices like laptops and smartphones [24]. Their benefits—self-configuration, cost efficiency, and flexibility—make them useful in disaster response, military, healthcare, and rural broadband [25], [26], [27].

A key WMN use case is fixed wireless access (FWA), which offers connectivity where cabling is infeasible. FWAs use distribution nodes (DNs) to provide access, with client nodes (CNs) acting as indoor APs. mmWave mesh networks also enable FWA, forming a distribution access network as shown in Fig. 14.

Today, Wi-Fi (IEEE 802.11) is the dominant indoor communication tech, linking various end devices. However, traffic loads vary widely, peaking during the day and dropping at night. Even when demand is low, APs and DNs remain fully active, wasting energy. To solve this, we propose a coordinated sleep schedule to reduce total network energy use.

Our solution applies periodic, dynamic schedules to all network nodes. Every 200 ms, traffic load is evaluated and node schedules updated accordingly. Fig. 15 shows initial Wi-Fi and DN schedules. Longer sleeping slots are feasible for mmWave nodes due to their higher data rates. Additionally, using in-band telemetry, time-sensitive applications are allocated dedicated slots, while best-effort apps use the remaining air-time.

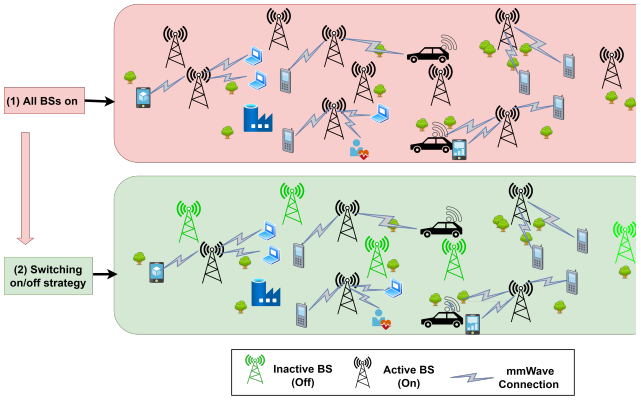

FIGURE 17. Illustration of μBS switching on/off strategy.

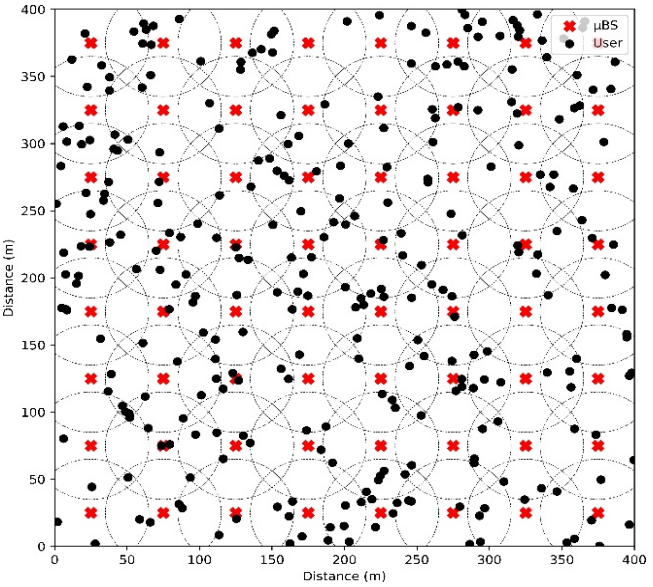

FIGURE 18. Illustration of the considered network configuration considering 64 μBSs and 300 users.

In our setup, we evaluated 4 voice (time-critical, TC), 4 TC video, and 7 best-effort applications. Results compare vanilla Wi-Fi versus Wi-Fi with scheduling. Vanilla Wi-Fi showed 71% idle time, where nodes were in listening mode. Our scheduling reduced this: APs reached 42% sleep time, DNs 62%, cutting energy use without impacting service. As Fig. 16 shows, energy savings reached 13% for APs and 33% for DNs.

B. Energy efficient network resource allocation

Dense deployment of mmWave μBSs is an important part of meeting 6G capacity demands [28], [29]. However, mmWave signals need more power than lower frequencies to cover the same area, leading to higher energy use and CO_2 emissions [30]. Given that the ICT sector already accounts for 4.7% of global electricity use and BSs can consume up to 80% of wireless network energy [31], improving energy efficiency is crucial. One approach to address the energy efficiency challenge is μBS on/off switching, which toggles nodes between active and sleep modes based on traffic to reduce power use [32]. Fig. 17 shows an example of user allocation under this strategy. We have explored joint user and power allocation in 6G mmWave networks, modeled as an ILP

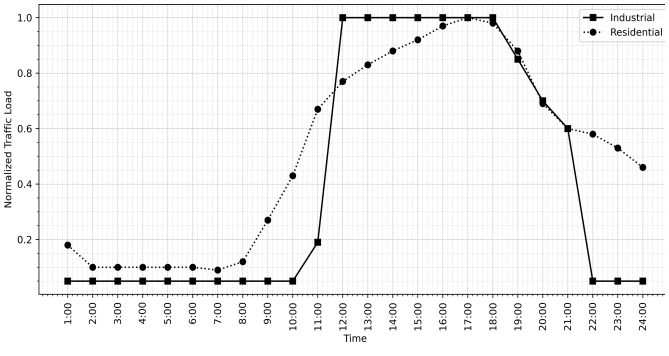

FIGURE 19. The considered residential and office traffic profiles.

This article has been accepted for publication in IEEE Open Journal of the Communications Society. This is the author's version which has not been fully edited and content may change prior to final publication. Citation information: DOI 10.1109/OJCOMS.2026.3707318

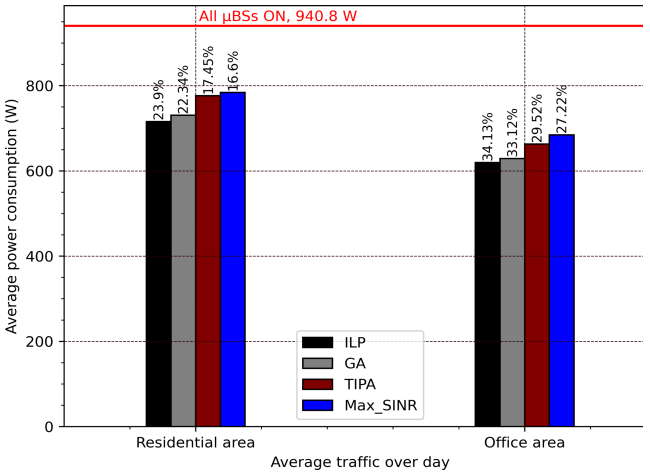

FIGURE 20. The average power consumption vs. the average daily traffic in the residential area and office area.

problem under QoS constraints. An energy-efficient GA solves this while incorporating μBS on/off control, with simulations showing that the GA performs near-optimally and surpasses benchmark methods like TIPA and Max-SINR [28].

1) Network Model: We again consider here a 400m×400m 6G mmWave grid with μBSs $\mathcal{S}$ indexed by $s \in 1, \ldots, S$, operating in either active (transmit) or inactive (sleep) mode. Users $u \in 1, \ldots, U$ are uniformly distributed (see Fig. 18), with all nodes assumed to have single omnidirectional antennas.

2) Traffic Model: We evaluated two traffic profiles: residential and office, as shown in Fig.19. Users are evenly distributed, and their access activity follows a Poisson process. Peak hours are 4:00–6:00p.m. in residential areas and 12:00–6:00 p.m. in office environments.

3) Simulation Results: Fig.20 shows average power use over 24 hours. In residential areas, the ILP algorithm achieves 715.9W (23.9% savings vs always-on), while the GA hits 730.6 W (22.3% savings). Max-SINR and TIPA trail with only

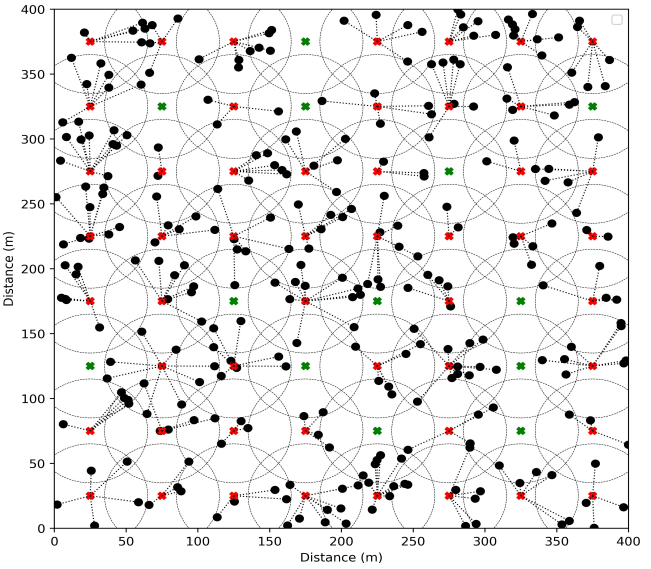

FIGURE 21. Example of users-μBSs assignment configuration in the case of 300 users.

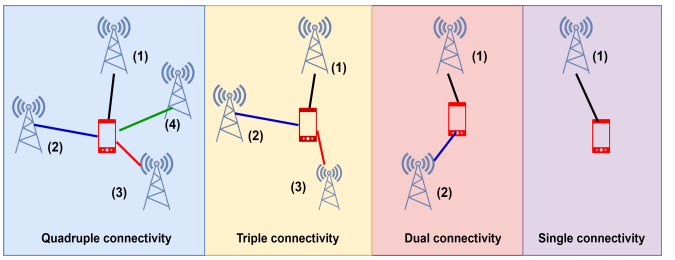

FIGURE 22. Illustration of the considered user multi-connectivity scenarios.

16.6% and 17.5% savings, respectively. In the office scenarios, the ILP leads with 619.7W (34.1% savings), GA follows at 629.2W (33.1% savings), then TIPA (663.0W, 29.5%) and Max-SINR (684.7W, 27.2%). Fig. 21 illustrates the user-to-μBS allocation under GA optimisation for 300 users. Black dots = users; red Xs = active μBSs; green Xs = inactive μBSs.

4) On the impact of the multi-connectivity on the network power consumption: Due to mmWave's path loss and blockage sensitivity, user multi-connectivity—simultaneous links to multiple BSs—improves reliability and performance [33]. However, energy management is made more complicated due to the dynamic loads and varied energy demands [34], [35], [36]. We therefore propose a dynamic multi-objective ILP to optimize power usage across four connectivity levels: single through to quadruple (Fig. 22).

In this work we consider a non-uniform user geographical distribution as shown in Fig 23. Figure 24 illustrates the count of μBSs (from a total of 64) that are deactivated under varying user densities and connectivity configurations. The data indicates that the highest number of μBSs are switched off in the single connectivity setup, followed in order by dual, triple, and then quadruple connectivity. While the single and dual

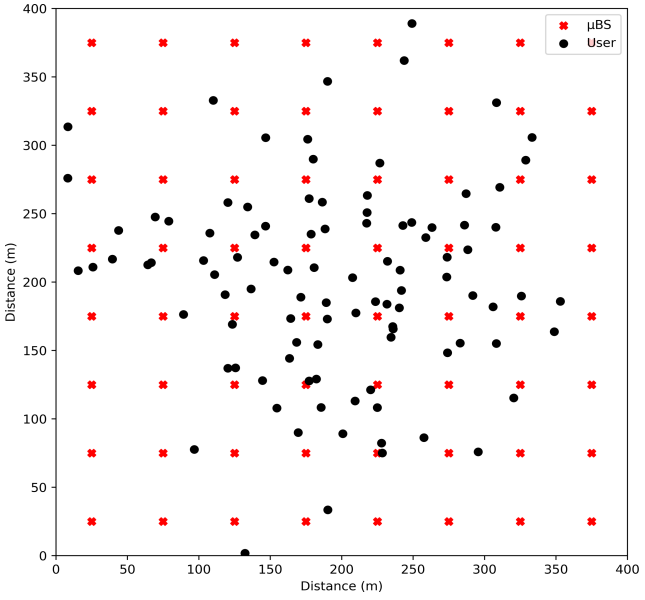

FIGURE 23. Example of the considered nonuniform user distribution for the case of 100 users.

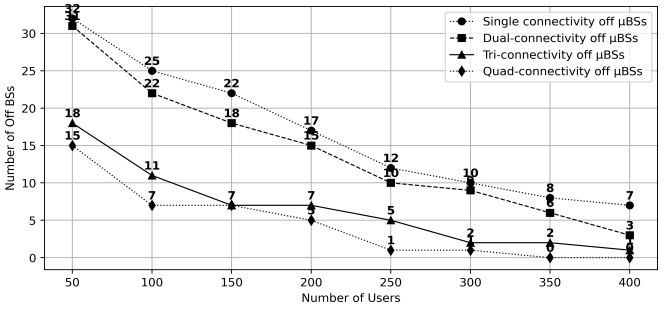

FIGURE 24. Number of switched off μBSs for different numbers of users.

connectivity results are close in magnitude, the transition to triple and quadruple connectivity leads to a marked decrease in the number of deactivated μBSs.

Fig. 25 compares the energy efficiencies across connection levels, where we find that for <100 users, performance is similar. As user count rises, single connectivity proves most energy- efficient, highlighting the trade-offs between redundancy and power use. Fig. 26 shows the diurnal traffic load characteristics that underpin the calculated average daily network powers by connectivity level, depicted in Fig.27, indicated by, Single: 352.0W; Dual: 422.3W; Triple: 444.4W; Quadruple: 451.1 W. Fig. 28 shows user-μBS mapping for 100 users with different connectivity levels. Red = active μBSs, green = inactive, black lines = links.

IV. USE CASE: ENERGY-EFFICIENT RESOURCE ALLOCATION

Miniature UAVs provide adaptable wireless coverage in confined or remote areas. However, their limited battery and high-frequency signal attenuation (e.g., mmWave or sub-THz) make energy efficiency (EE) a key challenge. The inclusion of Simultaneous Wireless Information and Power Transfer (SWIPT) and Non-Orthogonal Multiple Access (NOMA) further complicates resource management. This makes the scenario ideal for evaluating SAMBAS energy-saving and harvesting strategies [37]. Here we propose a joint optimization framework to maximize EE in a THz-enabled UAV relay under the tough energy and transmission constraints associated with high frequency operation.

As shown in Fig. 29, the system includes a ground source, a miniature UAV as an energy- harvesting relay, and a destination. The UAV operates in two phases: harvesting

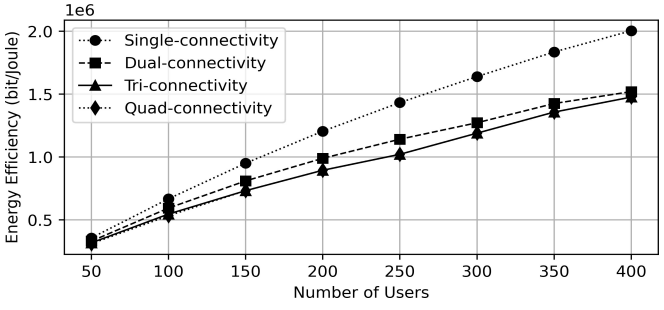

FIGURE 25. Network energy efficiency vs users connectivity for different numbers of users.

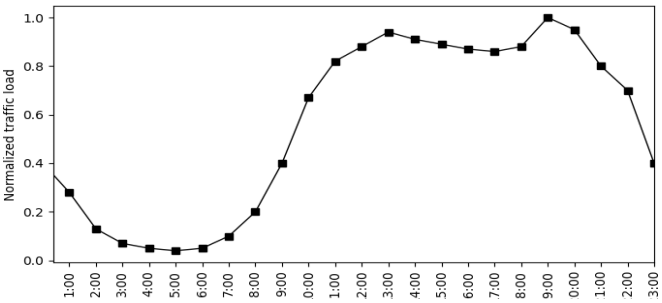

FIGURE 26. The considered normalized traffic load.

energy and decoding a NOMA signal, then relaying data using harvested energy. Optimization focuses on: 1) NOMA power allocation, 2) SWIPT power splitting, and 3) UAV trajectory.

We model this as a fractional non-convex optimization problem, solved in two stages: trajectory and power splitting (PS) ratios via successive convex approximation, and NOMA coefficients via quadratic transformation and Lagrangian methods.

1) Miniature UAV Network Setup and Parameters: The experimental setup consisted of a 30 m × 30 m indoor space with a UAV flying at 3 m height. The high-frequency carrier is 1.2 THz with 10 GHz bandwidth, featuring a path-loss molecular absorption coefficient $\xi = 0.005$ $m^{-1}/1000$ (at typical indoor humidity). UAV flight time is 45 s, max speed is 1 m/s. Noise power density is −174 dBm/Hz, UAV circuit power is 0.52 W, while the transmit power is capped at 1 W (peak and average).

2) Energy Efficiency vs. Network Transmit Power: Figure 30 shows the energy efficiency (Mbit/Joule) vs. average network transmit power $\bar{p}_{\text{sum}}$, comparing:

- **Initial:** Feasible initialization with a predefined UAV trajectory;
- **Method A:** Fixed NOMA power coefficients;
- **Method B:** Orthogonal Multiple Access (OMA) instead of NOMA;
- **Method C:** UAV follows a fixed trajectory;
- **Method D:** Constant power splitting (PS) SWIPT ratio set to 0.5 for all time slots;
- **Method E:** Fractional programming-based method without PS optimization.

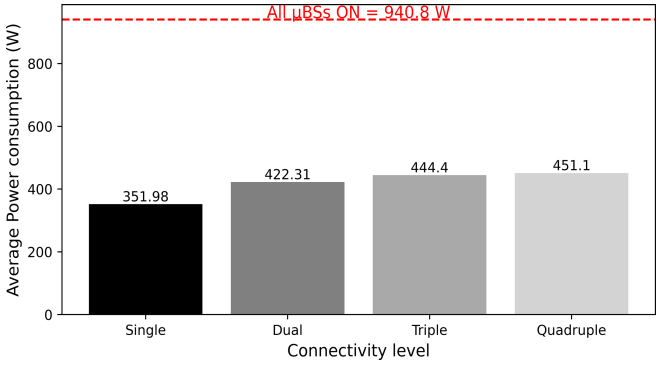

FIGURE 27. The impact of the connectivity scheme on the network power consumption over 24 hours of operation.

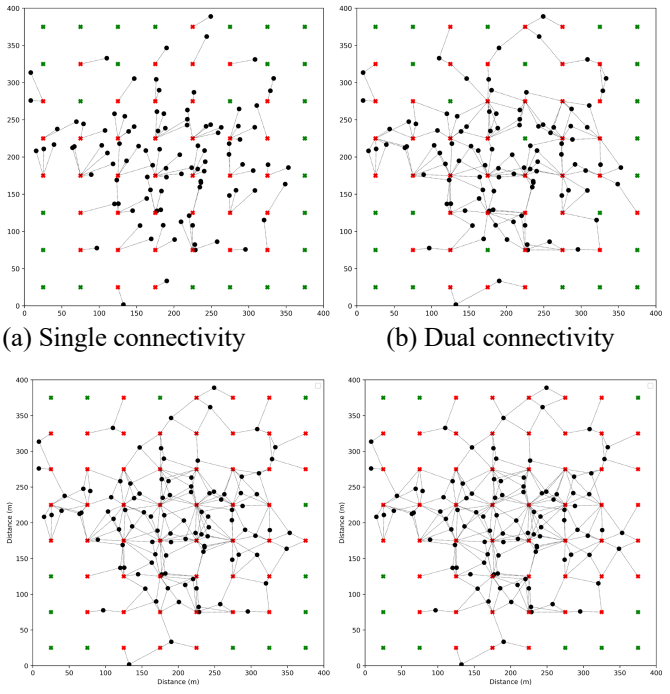

FIGURE 28. Example of users-μBSs assignment with single, dual, triple, and quadruple connectivities for 100 users.

Our method improves EE by up to 30.3 % over the initial setup, and outperforms all others: 23.0 % over A, 21.2 % over B, 18.1 % over C, 7.26 % over D, and 3.57 % over method E—showing the benefits of jointly optimizing all variables, especially in the energy-limited UAV context.

3) Optimized UAV Trajectory: Fig. 31 depicts the optimized 2D UAV paths. Unlike static or heuristic routes, the UAV maintains line-of-sight to the destination—crucial in THz bands where small shifts impact signal quality due to directivity and molecular loss.

4) Impact of Molecular Absorption on Energy Efficiency of the miniature UAV Network: Fig. 32 shows how the energy efficiency [Mb/J] drops as the molecular absorption coefficient increases (e.g., under high humidity). Despite this,

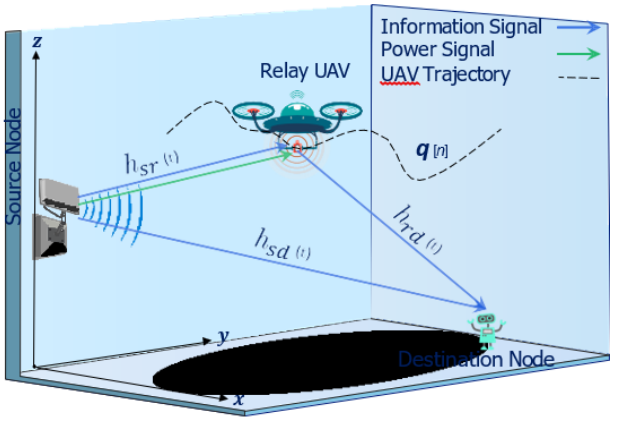

FIGURE 29. Miniature UAV-assisted cooperative NOMA-SWIPT network.

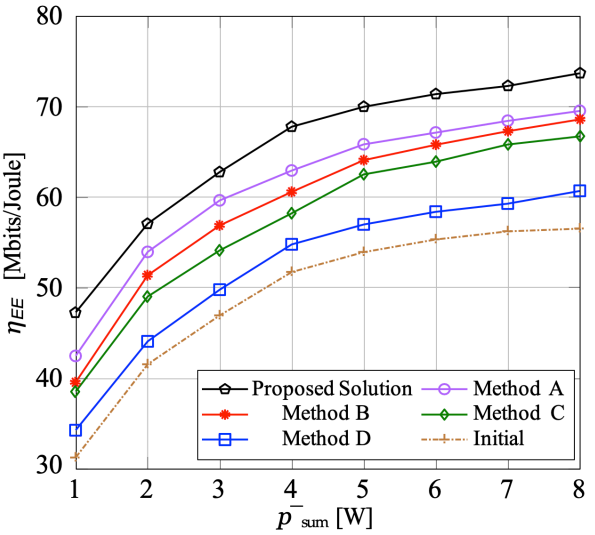

FIGURE 30. EE users vs. p_{sum}.

the proposed SAMBAS approach maintains the best EE performance, confirming its resilience to the harsh THz propagation conditions, and demonstrating that it is well-suited for indoor and humid environments where traditional schemes degrade more severely.

adapts its flight to reduce path loss and maximize energy harvesting. It moves closer to the source during harvesting and

V. CONCLUSIONS

In this paper, we have demonstrated consistent energy savings in 6G wireless networks using strategies applied at user devices, RAN equipment, and protocol levels. Notably, we have shown how AI can optimize energy harvesting and storage for micro base stations (μBSs), supporting dense indoor/outdoor 6G coverage while maintaining performance in reliability, latency, and throughput.

Within the SAMBAS project, where such technologies were tested, AI-optimized solar harvesting with local batteries

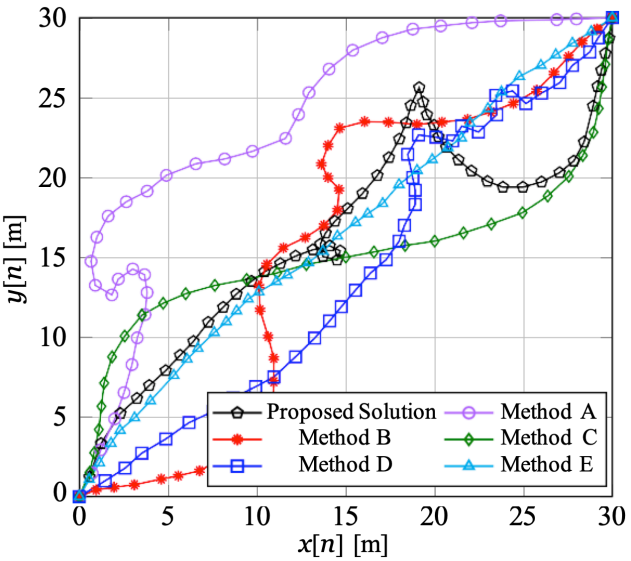

FIGURE 31. UAV trajectories.

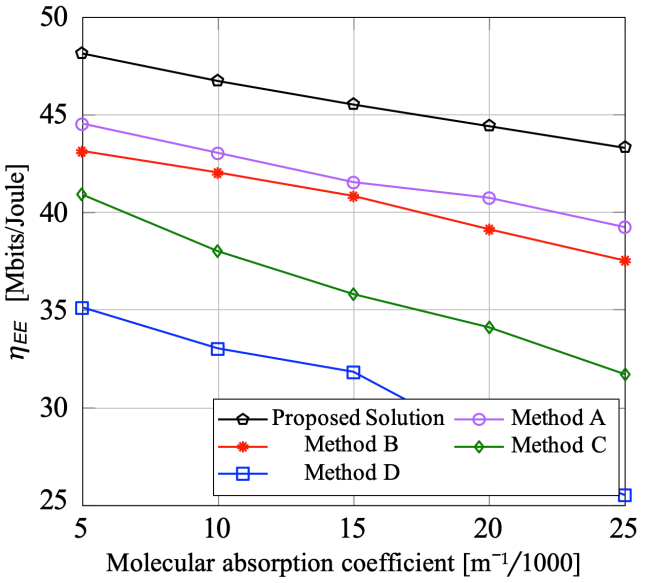

FIGURE 32. EE vs. Molecular absorption coefficient. trajectories.

achieved 15–20% energy savings without degrading performance. MAC protocol optimization during low traffic periods yielded 10–15% savings. For mmWave µBS devices, we observed a 24.5% saving while using the high-performance MCS 12 protocol. AI-driven energy prediction models can also optimize SAMBAS operations, with renewables reducing dependence on the grid and improving sustainability.

Network-wide energy savings through coordination of dense µBS deployments are also feasible. Optimizing interactions among µBSs—Distribution Nodes (DNs) outdoors, Access Points (APs) indoors—enabled 13% savings in indoor networks and up to 33% outdoors. The SAMBAS study used genetic algorithms (GAs) to achieve 22.3–33.1% savings based on indoor (office) or outdoor (residential) use cases. Applying SAMBAS principles to a cooperative UAV-relay 6G scenario using SWIPT also yielded up to 30.3% energy efficiency improvement.

In summary, even while satisfying the demanding performance requirements of 6G, we have demonstrated that significant energy-efficiency improvements and sustainable solutions are achievable. SAMBAS has shown that dense µBS networks powered by renewables and adopting intelligent networking technologies can deliver 6G performance while not costing the Earth.

REFERENCES

[1] P. Cochrane, "Where is wireless going?" ITP Journal, 2020.

[2] M.J. Shehab, et al., "5G Networks Towards Smart and Sustainable Cities: A Review of Recent Developments, Applications and Future Perspectives", IEEE Access, 10, 2987, 2022

[3] Z. Chen, et al., "Fundamental Trade-offs on Green Wireless Networks," IEEE Communications Magazine, 2011.

[4] M.C. Parker, S.D. Walker, "Roadmapping ICT: An Absolute Energy Efficiency Metric", Journal of Optical Communications and Networks, vol.3(8), pA49-A58, 2011

[5] G.Y. Li et al., "Energy-efficient wireless communications: Tutorial, survey, and open issues," IEEE Wireless Communications, 18(6), 28, 2011.

[6] D. Feng et al., "A Survey of Energy-Efficient Wireless Communications," IEEE Communications Surveys & Tutorials, 15(1), 167, 2012.

[7] S. Buzzi et al., "A Survey of Energy-Efficient Techniques for 5G Networks and Challenges Ahead," IEEE JSAC, 34(4), 697, 2016

[8] H.Q. Ngo, E.G. Larsson, T.L. Marzetta, "Energy and Spectral Efficiency of Very Large Multiuser MIMO Systems," IEEE Transactions on Communications, 61(4), 1436, 2013.

[9] D.S. Han, C. Yang, A.F. Molisch, "Spectrum and Energy Efficient Cooperative Base Station Doze," IEEE JSAC, 32(2), 285, 2014.

[10] J. Wu et al., "Energy-Efficient Base-Stations Sleep-Mode Techniques in Green Cellular Networks: A Survey," IEEE Communications Surveys & Tutorials, 17(2), 803, 2015.

[11] Y. Shi, J. Zhang, K.B. Letaief, "Group Sparse Beamforming for Green Cloud-RAN," IEEE Transactions on Wireless Communications, 13(5), 2809, 2014.

[12] H.Q. Ngo et al., "On the Total Energy Efficiency of Cell-Free Massive MIMO," IEEE Transactions on Green Communications and Networking, 2(1), 25, 2017.

[13] C. Huang et al., "Reconfigurable Intelligent Surfaces for Energy Efficiency in Wireless Communication," IEEE Transactions on Wireless Communications, 18(8), 4157, 2019.

[14] X. Lu et al., "Wireless Networks With RF Energy Harvesting: A Contemporary Survey," IEEE Communications Surveys & Tutorials, 17(2), 757, 2015.

[15] S. Ulukus et al., "Energy Harvesting Wireless Communications: A Review of Recent Advances," IEEE JSAC, 33(3), 360, 2015. [2] A. Research and Interdigital. (2020) Environmentally sustainable 5G deployment.

[16] T. S. Muratkar, A. Bhurane, and A. Kothari, "Battery-less internet of things – a survey," Computer Communications, vol. 180, 2020.

[17] B. Zahnstecher, "The 5G energy gap – a fatal flow for 5G deployment," IEEE Future Networks – Podcasts, 2020. [Online]. Available: https://futurenetworks.ieee.org/podcasts/the-5g-energy-gap

[18] A. Fayad, T. Cinkler, and J. Rak, "Toward 6G optical fronthaul: A survey on enabling technologies and research perspectives," IEEE Communications Surveys Tutorials, vol. 27, no. 1, pp. 629–666, 2025.

[19] A. Fayad, T. Cinkler, and J. Rak, "5G/6G optical fronthaul modeling: Cost and energy consumption assessment," Journal of Optical Communications and Networking, vol. 15, no. 9, pp. D33–D46, 2023.

[20] H. Assasa, N. Grosheva, T. Ropitault, S. Blandino, N. Golmie, and J. Widmer, "Implementation and evaluation of a WLAN IEEE 802.11ay model in network simulator ns-3," in Proceedings of the Workshop on NS-3 (WNS3), 2021.

[21] S. Mangiante, G. Klas, A. Navon, Z. GuanHua, J. Ran, and M. D. Silva, "VR is on the edge: How to deliver 360° videos in mobile networks," in Proceedings of the Workshop on Virtual Reality and Augmented Reality Network, 2017.

[22] B. Mao, F. Tang, Y. Kawamoto, and N. Kato, "AI models for green communications towards 6G," IEEE Communications Surveys & Tutorials, vol. 24, no. 1, pp. 210–247, 2021.

[23] A. Ladanyi and T. Cinkler, "Resilience–throughput–power trade-off in future 5g photonic networks," Photonic Network

Communications, vol. 37, pp. 296–310, 2019.

[24] K. Karthika, "Wireless mesh network: A survey," in 2016 international conference on wireless communications, signal processing and networking (WiSPNET). IEEE, 2016, pp. 1966–1970.

[25] I. F. Akyildiz, X. Wang, and W. Wang, "Wireless mesh networks: a survey," Computer networks, vol. 47, no. 4, pp. 445–487, 2005.

[26] S. M. Taleb, Y. Meraihi, A. B. Gabis, S. Mirjalili, and A. Ramdane-Cherif, "Nodes placement in wireless mesh networks using optimization approaches: a survey," Neural Computing and Applications, vol. 34, no. 7, pp. 5283–5319, 2022.

[27] M. I. Hussain, N. Ahmed, M. Z. I. Ahmed, and N. Sarma, "QoS provisioning in wireless mesh networks: A survey,"
Wireless Personal Communications, vol. 122, no. 1, pp. 157–195, 2022.

[28] A. Fayad and T. Cinkler, "Energy-efficient joint user and power allocation in 5G millimeter wave networks: A genetic algorithm-based approach," IEEE Access, vol. 12, pp. 20 019–20 030, 2024.

[29] A. Fayad and T. Cinkler, "Optimal slicing of mmwave micro base stations for 5G and beyond," Journal of Networking and Network Applications, vol. 3, no. 3, pp. 99–108, 2023.

[30] D. Moltchanov, E. Sopin, V. Begishev, A. Samuylov, Y. Koucheryavy, and K. Samouylov, "A tutorial on mathematical modeling of 5G/6G millimeter wave and terahertz cellular systems," IEEE Communications Surveys & Tutorials, vol. 24, no. 2, pp. 1072–1116, 2022.

[31] E. Gelenbe and Y. Caseau, "The impact of information technology on energy consumption and carbon emissions," ubiquity, vol. 2015, no. June, pp. 1–15, 2015.

[32] M. Feng, S. Mao, and T. Jiang, "Base station on-off switching in 5G wireless networks: Approaches and challenges,"
IEEE Wireless Communications, vol. 24, no. 4, pp. 46–54, 2017.

[33] T. Sylla, L. Mendiboure, S. Maaloul, H. Aniss, M. A. Chalouf, and S. Delbruel, "Multi-connectivity for 5G networks and beyond: A survey," Sensors, vol. 22, no. 19, p. 7591, 2022.

[34] A. Fayad and T. Cinkler, "Power consumption optimization in 5G/6G mmwave networks with user multi-connectivity," in
2024 IEEE Pacific Rim Conference on Communications, Computers and Signal Processing (PACRIM), 2024, pp. 1–6.

[35] A. Fayad, T. Cinkler, and J. Rak, "5G millimeter wave network optimization: Dual connectivity and power allocation strategy," IEEE Access, vol. 11, pp. 82 079–82 094, 2023.

[36] M.-T. Suer, C. Thein, H. Tchouankem, and L. Wolf, "Multi-connectivity as an enabler for reliable low latency communications—an overview," IEEE Communications Surveys & Tutorials, vol. 22, no. 1, pp. 156–169, 2019.

[37] J. Jalali, A. Khalili, H. Tabassum, R. Berkvens, J. Famaey, and W. Saad, "Energy-efficient THz NOMA for SWIPT-aided miniature UAV networks," IEEE Communications Letters, vol. 28, no. 5, pp. 1107–1111, 2024.

MICHAEL C. PARKER (Senior Member, IEEE) has over 30 years academic and industry experience researching photonics and wireless communications technologies. He has pioneered many important telecoms technologies, including the invention (during his doctoral research at Cambridge University) of liquid crystal on silicon (LCoS) technologies for high-resolution holographic flexgrid (WDM) wavelength control in optical telecommunications. Dr Parker has performed research into the foundations of information theory, applying thermodynamic principles to the theory of computation and communications, and provided fundamental
insights into technology solutions to minimize energy consumption. He has also applied his knowledge to 6G wireless networking and to cryptographic wireless quantum communications systems. He was appointed Visiting Professor at University of Essex (2004-2007) and since 2018 is a Visiting Fellow. Dr Parker has published over 170 papers in peer-reviewed journals and conferences, filed 25 patents, is a Chartered Engineer (CEng) with the IET and is also a Senior Member of the IEEE (SMIEEE).

GEZA KOCZIAN is a Senior Research Officer at the School of Computer Science and Electronic Engi- neering, University of Essex, and a part-time PhD researcher. His work advances sustainable wireless communications, energy-aware ICT, and intelligent data-driven systems. Geza is currently focused on the CircuBatt H2020 project, integrating artificial intelligence and big data analytics to enhance circularity and energy efficiency in battery systems. He previously contributed to the SAMBAS project, pioneering renewable-powered millimeter wave micro base stations. With over a decade of academic experience,
Geza has played key roles in major EU and UK programmes, including CHARISMA, iCIRRUS, and NIRVANA, and led the design of the world's first rail-approved 10/40Gb/s Ethernet inter-car connectivity systems. He is committed to bridging research and innovation for resilient, sustainable, and intelligent digital infrastructure.

MANOJ THAKUR received the B.E. degree in Electronics and Communication Engineering from BIT Mesra, India, in 2000, and the Ph.D. degree in optical access networks from the University of Essex, U.K., in 2009. He has held research and academic positions at Schindler EE, Nortel Labs (TCS), AMEX, University of Essex, University College London (UCL), and the University of Hertfordshire. At UCL, he established and managed the CONNET and Aeroflex laboratories and played a key role in the U.K.'s National Dark Fibre Infrastructure Service (NDFIS). He is currently an academic at the University of Essex and part
of The Access Networks Group (ANG). His research focuses on radio-over-fiber systems for next-generation access networks, passive optical networks, photonic millimetre-wave generation, energy-efficient MAC/PHY integration, and IoT/Mechatronics sensor systems. He has contributed to numerous EU and U.K.-funded projects and published widely in journals and conferences. He has led international collaborations and supported several successful grant proposals.

NABEEL NISAR BHAT is a Ph.D. researcher in the field of Joint Communication and Sensing at the IDLab research group (University of Antwerp) and imec research institute, Belgium. He obtained his M.Sc. (2021) in Communications and Computer Networks Engineering at Politecnico di Torino. His current research focuses on leveraging mmWave communication signals for pose estimation in Extended Reality applications. He has experience in signal processing, wireless communications, and deep learning.

JAKOB STRUYE is a postdoctoral researcher in the field of wireless networking at the IDLab research group (University of Antwerp) and imec research institute, Belgium. He obtained his M.Sc. (2017) and Ph.D. (2024) in Computer Science at the University of Antwerp. His current research focuses on leveraging extremely high frequency wireless networks in the millimeter-wave bands to improve the performance of truly wireless Virtual and Augmented Reality experiences, and he has experience in applying Artificial Intelligence to time series prediction problems.

PLACE PHOTO HERE

JOSHUA JALALI holds a PhD from the University of Antwerp and currently works as a factory worker. In his personal time, he contributes to the scientific community, serving as a reviewer and TPC for IEEE.

PLACE PHOTO HERE

OZGUR OZKAYA received his bachelor's and master's degrees in computer engineering from Yalova University, Türkiye in 2019. He is currently pursuing a PhD degree at Ghent University - imec in deterministic wireless communication

PLACE PHOTO HERE

JETMIR HAXHIBEQIRI received the Masters degree in Engineering (information technology and computer engineering) from RWTH Aachen University, Germany (2013). In 2019, he obtained a Ph.D. in Engineering Computer Science from Ghent University with his research on flexible and scalable wireless communication solutions for industrial warehouses and logistics applications. Currently he is a senior researcher in the Internet Technology and Data Science Lab (IDLab) of Ghent University and imec. His current research interests include wireless communications technologies (IEEE 802.11, IEEE 802.15.4e, LoRa) and their application, IoT, wireless time sensitive networking, in-band network monitoring and wireless network management.

ABDULHALIM FAYAD received his Ph.D. in Electrical Engineering from the Budapest University of Tech- nology and Economics, Hungary, in 2024. He earned his M.Sc. in Advanced Communication Engineering from Damascus University, Syria, in 2019. He is currently a Research Fellow at the HSN Laboratory, Department of Telecommunications and Artificial Intelligence (TMIT), Budapest University of Technology and Economics. He is also a member of the HUN-REN–BME Network Cloud Applications Research Group.
His research interests include communication network optimization, energy efficiency, green communications, network slicing, optical access networks, Xhaul design for 5G/6G, and resource allocation for mmWave wireless networks beyond 5G.

STUART D. WALKER received the B.Sc. (Hons) degree in physics from Manchester University, U.K., in 1973, the M.Sc. degree in telecommunications systems and Ph.D. degree in electronics from Essex University, Colchester, U.K., in 1975 and 1981 respectively. From 1981-82, he was a post-doctoral research assistant at Essex University. From 1982- 87, he was a research scientist at BT Laboratories, and from 1987-88 he was promoted to Group Leader in Submarine Systems Design. He joined Essex University in 1988 as a Senior Lecturer, and was promoted to Reader in 2002 and to Full Professor in 2004. At Essex University, he manages a laboratory concerned with all aspects of Access Networks: The Access Networks Group (ANG).

PLACE PHOTO HERE

JEROEN HOEBEKE received the master's degree in engineering computer science from Ghent University, in 2002, and the Ph.D. degree in engineering computer science, in 2007, with his research on adaptive ad hoc routing and virtual private ad hoc networks. He is currently an Associate Professor with the Internet Technology and Data Science Laboratory, Ghent Universityimec. He is the author or co-author of more than 200 publications in international journals or conference proceedings. He is conducting and coordinating research on wireless (IoT) connectivity, embedded communication stacks, deterministic
wireless communication, and wireless network management.

TIBOR CINKLER received his M.Sc. and Ph.D. degrees from the Budapest University of Technology and Economics (BME), Hungary, in 1994 and 1999, respectively. He habilitated at BME in 2013 and earned his D.Sc. degree from the Hungarian Academy of Sciences the same year.
He is currently a Full Professor at the Department of Telecommunications and Artificial Intelligence at BME. He has authored over 300 peer-reviewed scientific publications, including four patents, with nearly 3,000 citations at https://scholar.google.com/citations?user= ZI8D1UAAAAJ&hl=en.
His research focuses on the optimization of communication networks, including optical networks, 5G/6G cellular mobile networks, IoT/IIoT, and non-terrestrial networks (NTN), with a particular emphasis on energy efficiency and high availability.

JEROEN FAMAEY is an associate research professor at the Department of Computer Science of the University of Antwerp and imec, Belgium. His research focuses on performance modeling and optimization of wireless network protocols. He has published over 200 peer-reviewed journal articles and conference papers, and 8 granted patents. He was listed as one of the top 2% most cited scientists worldwide by Stanford University both in 2022 and 2023.